Supporting Information

Probing proline residues in the prokaryotic ligand-gated ion channel, ELIC.

Richard Mosesso[1], Dennis Dougherty[1], Sarah C. R. Lummis[2*]

[1]Division of Chemistry and Chemical Engineering, California Institute of Technology, Pasadena, California 91125, USA. [2]Department of Biochemistry, University of Cambridge, Tennis Court Road, Cambridge CB2 1GA, UK.

Running title: Proline residues in ELIC

* Corresponding Author Sarah C.R. Lummis, sl120@cam.ac.uk

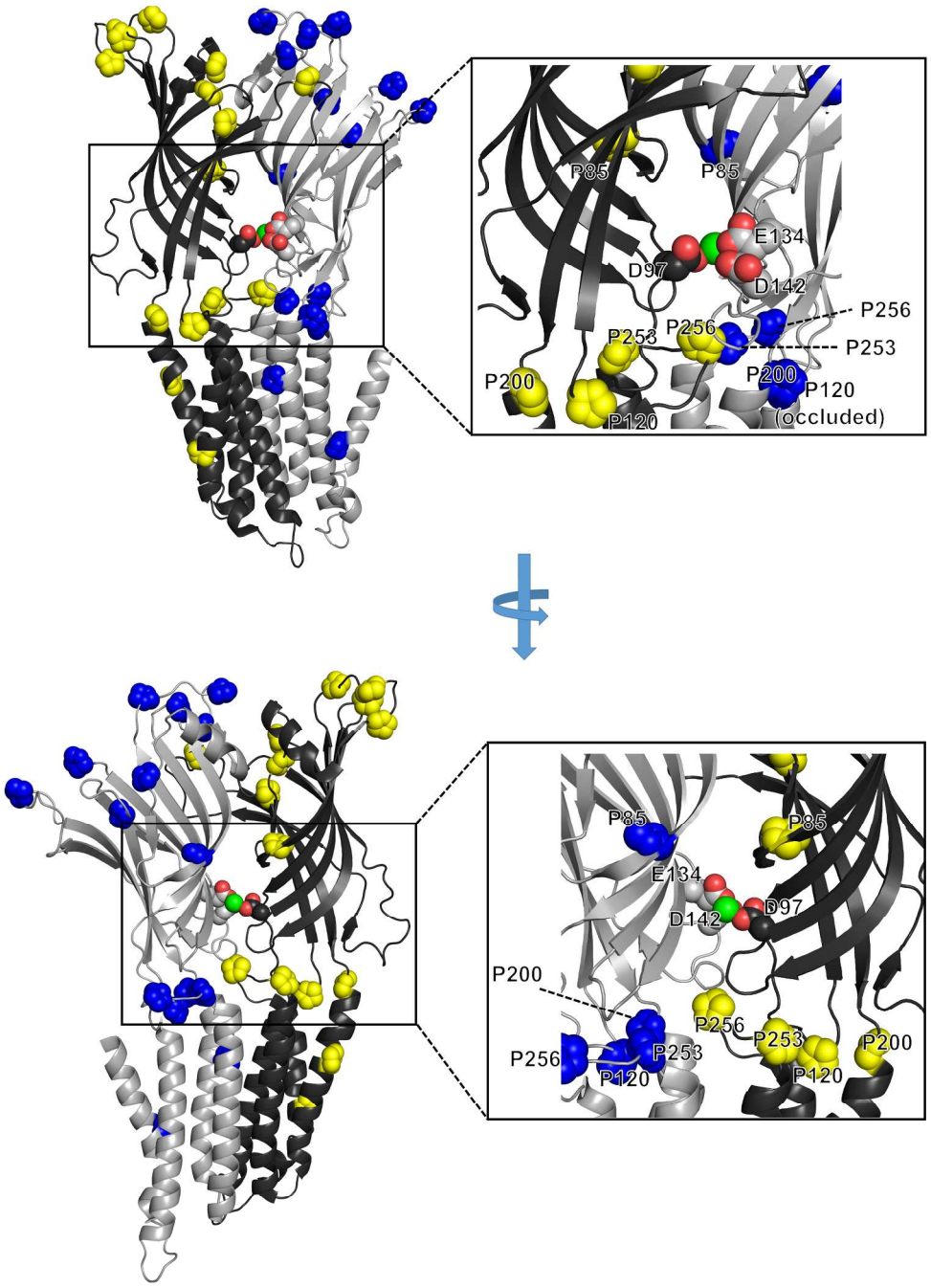

Figure S1. Divalent cation binding-site in ELIC, as exemplified by a crystal structure with Ba^{2+} (PDB 2YN6). Two subunits of the homopentamer are shown. The primary face is shown in light gray with Pro side chains in blue, while the complementary face is shown in black with Pros in yellow. Oxygen atoms on negatively-charged residues in the divalent cation binding site are shown in red, and the Ba^{2+} ion is shown in green. Additional Ba^{2+} atoms bind to different sites in this crystal structure, but the site illustrated in this figure was shown to be responsible for the modulatory effect of Ca^{2+}.[26]

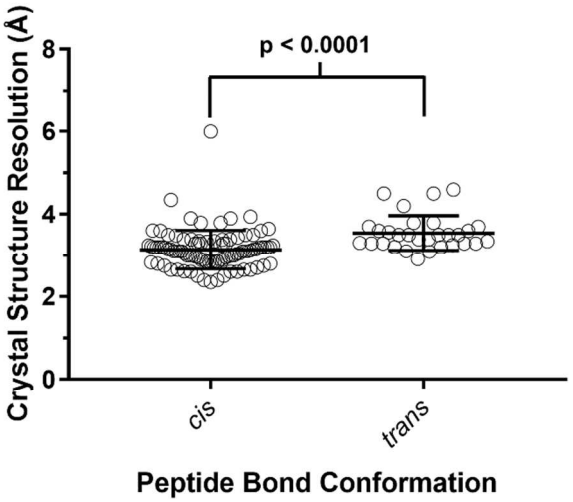

Figure S2. Correlation between crystal structure resolution and assignment of a *cis* peptide bond at the ß6-ß7 loop Pro in 124 X-ray crystal structures of pLGICs in the Protein Data Bank. Analysis of statistical significance was performed in GraphPad Prism using a nonparametric Mann-Whitney test.

Table S1. X-ray crystal structures of pLGICs used to analyze conformation of ß6-ß7 loop proline.[a]

PDB Code	Receptor	Resolution (Å)	ß6-ß7 Loop Pro Conformation	Citation
6F0U	GLIC E35A	2.35	cis	1
4HFI	GLIC	2.4	cis	2
4IL4	GLIC	2.4	cis	2
6F0R	GLIC E82Q	2.5	cis	1
6F0Z	GLIC D88N	2.5	cis	1
3TLW	GLIC - crosslinked	2.6	cis	3
5IUX	GLIC V135C	2.6	cis	Fourati et al, 2016 TBP
6F16	GLIC H277Q	2.6	cis	1
5TIN	GlyR α3 N38Q	2.61	cis	Huang et al, 2017 TBP
4HFH	GLIC	2.65	cis	4
5MZR	GLIC H235Q	2.65	cis	Fourati et al, 2018 TBP
5MZT	GLIC H235Q	2.65	cis	Fourati et al, 2018 TBP
6F0M	GLIC E35Q	2.65	cis	1
6F13	GLIC E75A	2.7	cis	1
4HFB	GLIC F14'A	2.75	cis	4
5OSA	GLIC-$GABA_AR$ chimera	2.75	cis	5
4HFE	GLIC	2.8	cis	4
5MZQ	GLIC M205W	2.8	cis	Fourati et al, 2018 TBP
4IL9	GLIC A237F	2.83	cis	2
3TLU	GLIC - crosslinked	2.85	cis	3
5VDH	GlyR α3	2.85	cis	6
6F0V	GLIC E82Q	2.85	cis	1
6F10	GLIC D88N	2.85	cis	1
6F15	GLIC H127Q	2.85	cis	1
3EAM	GLIC	2.9	cis	7
3TLV	GLIC - crosslinked	2.9	cis	3
3UU5	GLIC - crosslinked	2.9	cis	3
3UUB	GLIC - crosslinked	2.9	cis	3
5HCJ	GLIC	2.95	cis	8
6F11	GLIC D86A	2.95	cis	1
4COF	$GABA_A$ ß3	2.97	cis	9
3UU6	GLIC - crosslinked	2.98	cis	3
4F8H	GLIC	2.99	cis	10
4ILC	GLIC	2.99	cis	2
4QH5	GLIC	3	cis	11

4Z90	ELIC	3	cis	12
6F0I	GLIC E26A	3	cis	1
5CFB	GlyR a3	3.04	cis	13
3UU4	GLIC - crosslinked	3.05	cis	3
4HFC	GLIC F14'A	3.05	cis	4
4HFD	GLIC	3.1	cis	4
4ZZC	GLIC	3.1	cis	[14]
5MUR	GLIC F14'A	3.1	cis	Sauguet et al, 2018 TBP
5MVM	GLIC F14'A N15'A	3.1	cis	Fourati et al, 2018 TBP
5OSC	GLIC-$GABA_A$ chimera	3.1	cis	5
5SXU	ELIC	3.1	cis	15
5VDI	GlyR α3 N38Q	3.1	cis	6
5V6O	GLIC G2'L I9'A	3.12	cis	16
3UU3	GLIC - crosslinked	3.15	cis	3
4ILB	GLIC A237F	3.15	cis	2
5HCM	GLIC	3.15	cis	8
6F0J	GLIC E26A	3.15	cis	1
4IRE	GLIC with mutations in loop C	3.19	cis	17
5MUO	GLIC	3.19	cis	Fourati et al, 2017 TBP
3P4W	GLIC	3.2	cis	18
3TLS	GLIC E19'P	3.2	cis	3
4QH4	GLIC	3.2	cis	11
4TNW	GluCl	3.2	cis	19
4TWD	ELIC	3.2	cis	20
5O8F	GABAA ß3-α5 chimera	3.2	cis	21
6F0N	GLIC E82A	3.2	cis	1
6F12	GLIC E181A	3.2	cis	1
4LMK	GLIC Y27'A	3.22	cis	22
3UU8	GLIC - crosslinked	3.25	cis	3
5J0Z	GLIC	3.25	cis	Basak et al, 2017 TBP
5TIO	GlyR α3	3.25	cis	Huang et al, 2017 TBP
3P50	GLIC	3.3	cis	18
3TLT	GLIC H11'F	3.3	cis	3
5L47	GLIC	3.3	cis	23
5L4H	GLIC	3.3	cis	23
5OJM	GABAA ß3-α5 chimera	3.3	cis	21
4A97	ELIC	3.34	cis	24
4NPP	GLIC-His_{10}	3.35	cis	25
5V6N	GLIC C27S K33C I9'A N21'A	3.36	cis	16
4Z91	ELIC	3.39	cis	12

4QH1	GLIC	3.4	cis	11
4ZZB	GLIC	3.4	cis	14
5SXV	ELIC	3.4	cis	15
4LMJ	GLIC T25'A	3.44	cis	22
5MVN	GLIC M205W	3.49	cis	Fourati et al, 2017 TBP
4ILA	GLIC	3.5	cis	2
4X5T	GlyR-GLIC chimera	3.5	cis	26
5L4E	GLIC	3.5	cis	23
4TNV	GluCl	3.6	cis	19
4TWH	ELIC F16'S	3.6	cis	20
4A98	ELIC	3.61	cis	24
3ZKR	ELIC	3.65	cis	27
4LML	GLIC I9'A T25'A	3.8	cis	22
5OSB	GLIC-$GABA_A$ chimera	3.8	cis	5
2YOE	ELIC	3.9	cis	24
4TWF	ELIC	3.9	cis	20
5KXI	α4ß2 nAChR	3.94	cis	28
4NPQ	GLIC	4.35	cis	25
6F7A	GLIC	6	cis	29
3RQW	ELIC	2.91	trans	10
3RQU	ELIC	3.09	trans	10
3EHZ	GLIC	3.1	trans	30
2XQ9	GLIC E221A	3.2	trans	31
5HEG	GLIC P246G	3.21	trans	32
3RHW	GluCl	3.26	trans	33
2VL0	ELIC	3.3	trans	34
2YKS	ELIC F246A	3.3	trans	35
5HEH	GLIC P246G	3.3	trans	32
5HEO	ELIC P254G	3.3	trans	32
2YN6	ELIC	3.31	trans	36
3RIF	GluCl	3.35	trans	33
2XQ7	GLIC	3.4	trans	31
3RI5	GluCl	3.4	trans	33
2XQ3	GLIC	3.5	trans	31
2XQ5	GLIC	3.5	trans	31
3EI0	GLIC E221A	3.5	trans	34
4PIR	5-$HT3_A$	3.5	trans	37
5HEJ	ELIC F116A	3.5	trans	32
5LG3	ELIC	3.57	trans	38
2XQ4	GLIC	3.6	trans	31
2XQ8	GLIC	3.6	trans	31

2XQ6	GLIC	3.7	trans	31
2XQA	GLIC	3.7	trans	31
3RIA	GluCl	3.8	trans	33
3UQ7	ELIC L9'S F16'S	3.8	trans	39
3UQ5	ELIC L9'S F16'S	4.2	trans	39
5HEW	ELIC T28D	4.5	trans	32
5LID	ELIC	4.5	trans	38
4YEU	ELIC-GLIC chimera	4.6	trans	Chakrapani et al, 2015 TBP

[a] Crystal structures are grouped by *cis* and *trans* conformation about the ß6-ß7 prolyl peptide bond and listed in order of decreasing resolution. One pLGIC structure (3UQ4) was excluded from this analysis because it had an ambiguous, bent conformation about the prolyl peptide bond. Structures lacking a transmembrane domain were excluded from this analysis. TBP= to be published.

(1) Nemecz, Á., Hu, H., Fourati, Z., Renterghem, C. V., Delarue, M., and Corringer, P.-J. (2017) Full mutational mapping of titratable residues helps to identify proton-sensors involved in the control of channel gating in the Gloeobacter violaceus pentameric ligand-gated ion channel. *PLOS Biol. 15*, e2004470.

(2) Sauguet, L., Poitevin, F., Murail, S., Van Renterghem, C., Moraga-Cid, G., Malherbe, L., Thompson, A. W., Koehl, P., Corringer, P.-J., Baaden, M., and Delarue, M. (2013) Structural basis for ion permeation mechanism in pentameric ligand-gated ion channels. *EMBO J. 32*, 728–741.

(3) Prevost, M. S., Sauguet, L., Nury, H., Van Renterghem, C., Huon, C., Poitevin, F., Baaden, M., Delarue, M., and Corringer, P.-J. (2012) A locally closed conformation of a bacterial pentameric proton-gated ion channel. *Nat. Struct. Mol. Biol. 19*, 642–649.

(4) Sauguet, L., Howard, R. J., Malherbe, L., Lee, U. S., Corringer, P.-J., Harris, R. A., and Delarue, M. (2013) Structural basis for potentiation by alcohols and anaesthetics in a ligand-gated ion channel. *Nat. Commun. 4*, 1697.

(5) Laverty, D., Thomas, P., Field, M., Andersen, O. J., Gold, M. G., Biggin, P. C., Gielen, M., and Smart, T. G. (2017) Crystal structures of a $GABA_A$-receptor chimera reveal new endogenous neurosteroid-binding sites. *Nat. Struct. Mol. Biol. 24*, 977–985.

(6) Huang, X., Chen, H., and Shaffer, P. L. (2017) Crystal Structures of Human GlyRα3 Bound to Ivermectin. *Structure 0*.

(7) Bocquet, N., Nury, H., Baaden, M., Le Poupon, C., Changeux, J.-P., Delarue, M., and Corringer, P.-J. (2009) X-ray structure of a pentameric ligand-gated ion channel in an apparently open conformation. *Nature 457*, 111–114.

(8) Laurent, B., Murail, S., Shahsavar, A., Sauguet, L., Delarue, M., and Baaden, M. (2016) Sites of Anesthetic Inhibitory Action on a Cationic Ligand-Gated Ion Channel. *Structure 24*, 595–605.

(9) Miller, P. S., and Aricescu, A. R. (2014) Crystal structure of a human GABAA receptor. *Nature 512*, 270–275.

(10) Pan, J., Chen, Q., Willenbring, D., Mowrey, D., Kong, X.-P., Cohen, A., Divito, C. B., Xu, Y., and Tang, P. (2012) Structure of the Pentameric Ligand-Gated Ion Channel GLIC Bound With Anesthetic Ketamine. *Struct. Lond. Engl. 1993 20*, 1463–1469.
(11) Fourati, Z., Sauguet, L., and Delarue, M. (2015) Genuine open form of the pentameric ligand-gated ion channel GLIC. *Acta Crystallogr. D Biol. Crystallogr. 71*, 454–460.
(12) Chen, Q., Kinde, M. N., Arjunan, P., Wells, M. M., Cohen, A. E., Xu, Y., and Tang, P. (2015) Direct Pore Binding as a Mechanism for Isoflurane Inhibition of the Pentameric Ligand-gated Ion Channel ELIC. *Sci. Rep. 5*.
(13) Huang, X., Chen, H., Michelsen, K., Schneider, S., and Shaffer, P. L. (2015) Crystal structure of human glycine receptor-α3 bound to antagonist strychnine. *Nature 526*, 277–280.
(14) Sauguet, L., Fourati, Z., Prangé, T., Delarue, M., and Colloc'h, N. (2016) Structural Basis for Xenon Inhibition in a Cationic Pentameric Ligand-Gated Ion Channel. *PLoS ONE 11*.
(15) Chen, Q., Wells, M. M., Tillman, T. S., Kinde, M. N., Cohen, A., Xu, Y., and Tang, P. (2017) Structural Basis of Alcohol Inhibition of the Pentameric Ligand-Gated Ion Channel ELIC. *Structure 25*, 180–187.
(16) Gonzalez-Gutierrez, G., Wang, Y., Cymes, G. D., Tajkhorshid, E., and Grosman, C. (2017) Chasing the open-state structure of pentameric ligand-gated ion channels. *J. Gen. Physiol. 149*, 1119–1138.
(17) Mowrey, D., Chen, Q., Liang, Y., Liang, J., Xu, Y., and Tang, P. (2013) Signal Transduction Pathways in the Pentameric Ligand-Gated Ion Channels. *PLoS ONE 8*.
(18) Nury, H., Van Renterghem, C., Weng, Y., Tran, A., Baaden, M., Dufresne, V., Changeux, J.-P., Sonner, J. M., Delarue, M., and Corringer, P.-J. (2011) X-ray structures of general anaesthetics bound to a pentameric ligand-gated ion channel. *Nature 469*, 428–431.
(19) Althoff, T., Hibbs, R. E., Banerjee, S., and Gouaux, E. (2014) X-ray structures of GluCl in apo states reveal gating mechanism of Cys-loop receptors. *Nature 512*, 333–337.
(20) Ulens, C., Spurny, R., Thompson, A. J., Alqazzaz, M., Debaveye, S., Han, L., Price, K., Villalgordo, J. M., Tresadern, G., Lynch, J. W., and Lummis, S. C. R. (2014) The prokaryote ligand-gated ion channel ELIC captured in a pore blocker-bound conformation by the Alzheimer's disease drug memantine. *Struct. Lond. Engl. 1993 22*, 1399–1407.
(21) Miller, P. S., Scott, S., Masiulis, S., De Colibus, L., Pardon, E., Steyaert, J., and Aricescu, A. R. (2017) Structural basis for $GABA_A$ receptor potentiation by neurosteroids. *Nat. Struct. Mol. Biol. 24*, 986–992.
(22) Gonzalez-Gutierrez, G., Cuello, L. G., Nair, S. K., and Grosman, C. (2013) Gating of the proton-gated ion channel from Gloeobacter violaceus at pH 4 as revealed by X-ray crystallography. *Proc. Natl. Acad. Sci. U. S. A. 110*, 18716–18721.
(23) Fourati, Z., Ruza, R. R., Laverty, D., Drège, E., Delarue-Cochin, S., Joseph, D., Koehl, P., Smart, T., and Delarue, M. (2017) Barbiturates Bind in the GLIC Ion Channel Pore and Cause Inhibition by Stabilizing a Closed State♦. *J. Biol. Chem. 292*, 1550–1558.
(24) Spurny, R., Ramerstorfer, J., Price, K., Brams, M., Ernst, M., Nury, H., Verheij, M., Legrand, P., Bertrand, D., Bertrand, S., Dougherty, D. A., de Esch, I. J. P., Corringer, P.-J., Sieghart, W., Lummis, S. C. R., and Ulens, C. (2012) Pentameric ligand-gated ion channel ELIC is activated by GABA and modulated by benzodiazepines. *Proc. Natl. Acad. Sci. U. S. A. 109*, E3028–E3034.
(25) Sauguet, L., Shahsavar, A., Poitevin, F., Huon, C., Menny, A., Nemecz, À., Haouz, A., Changeux, J.-P., Corringer, P.-J., and Delarue, M. (2014) Crystal structures of a pentameric

ligand-gated ion channel provide a mechanism for activation. *Proc. Natl. Acad. Sci. 111*, 966–971.
(26) Moraga-Cid, G., Sauguet, L., Huon, C., Malherbe, L., Girard-Blanc, C., Petres, S., Murail, S., Taly, A., Baaden, M., Delarue, M., and Corringer, P.-J. (2015) Allosteric and hyperekplexic mutant phenotypes investigated on an α1 glycine receptor transmembrane structure. *Proc. Natl. Acad. Sci. U. S. A. 112*, 2865–2870.
(27) Spurny, R., Billen, B., Howard, R. J., Brams, M., Debaveye, S., Price, K. L., Weston, D. A., Strelkov, S. V., Tytgat, J., Bertrand, S., Bertrand, D., Lummis, S. C. R., and Ulens, C. (2013) Multisite Binding of a General Anesthetic to the Prokaryotic Pentameric Erwinia chrysanthemi Ligand-gated Ion Channel (ELIC). *J. Biol. Chem. 288*, 8355–8364.
(28) Morales-Perez, C. L., Noviello, C. M., and Hibbs, R. E. (2016) X-ray structure of the human α4β2 nicotinic receptor. *Nature 538*, 411–415.
(29) Zabara, A., Chong, J. T. Y., Martiel, I., Stark, L., Cromer, B. A., Speziale, C., Drummond, C. J., and Mezzenga, R. (2018) Design of ultra-swollen lipidic mesophases for the crystallization of membrane proteins with large extracellular domains. *Nat. Commun. 9*.
(30) Hilf, R. J. C., and Dutzler, R. (2009) Structure of a potentially open state of a proton-activated pentameric ligand-gated ion channel. *Nature 457*, 115–118.
(31) Hilf, R. J. C., Bertozzi, C., Zimmermann, I., Reiter, A., Trauner, D., and Dutzler, R. (2010) Structural basis of open channel block in a prokaryotic pentameric ligand-gated ion channel. *Nat. Struct. Mol. Biol. 17*, 1330–1336.
(32) Bertozzi, C., Zimmermann, I., Engeler, S., Hilf, R. J. C., and Dutzler, R. (2016) Signal Transduction at the Domain Interface of Prokaryotic Pentameric Ligand-Gated Ion Channels. *PLOS Biol 14*, e1002393.
(33) Hibbs, R. E., and Gouaux, E. (2011) Principles of activation and permeation in an anion-selective Cys-loop receptor. *Nature 474*, 54–60.
(34) Hilf, R. J. C., and Dutzler, R. (2008) X-ray structure of a prokaryotic pentameric ligand-gated ion channel. *Nature 452*, 375–379.
(35) Zimmermann, I., and Dutzler, R. (2011) Ligand Activation of the Prokaryotic Pentameric Ligand-Gated Ion Channel ELIC. *PLoS Biol 9*, e1001101.
(36) Zimmermann, I., Marabelli, A., Bertozzi, C., Sivilotti, L. G., and Dutzler, R. (2012) Inhibition of the Prokaryotic Pentameric Ligand-Gated Ion Channel ELIC by Divalent Cations. *PLOS Biol. 10*, e1001429.
(37) Hassaine, G., Deluz, C., Grasso, L., Wyss, R., Tol, M. B., Hovius, R., Graff, A., Stahlberg, H., Tomizaki, T., Desmyter, A., Moreau, C., Li, X.-D., Poitevin, F., Vogel, H., and Nury, H. (2014) X-ray structure of the mouse serotonin 5-HT3 receptor. *Nature 512*, 276–281.
(38) Nys, M., Wijckmans, E., Farinha, A., Yoluk, Ö., Andersson, M., Brams, M., Spurny, R., Peigneur, S., Tytgat, J., Lindahl, E., and Ulens, C. (2016) Allosteric binding site in a Cys-loop receptor ligand-binding domain unveiled in the crystal structure of ELIC in complex with chlorpromazine. *Proc. Natl. Acad. Sci.* 201603101.
(39) Gonzalez-Gutierrez, G., Lukk, T., Agarwal, V., Papke, D., Nair, S. K., and Grosman, C. (2012) Mutations that stabilize the open state of the Erwinia chrisanthemi ligand-gated ion channel fail to change the conformation of the pore domain in crystals. *Proc. Natl. Acad. Sci. U. S. A. 109*, 6331–6336.